Rev.Adv.Mater.Sci. 7 (2004) 97-107

SURFACE MODIFICATIONS OF NANOPARTICLES AND NANOTUBES BY PLASMA POLYMERIZATION

Donglu Shi and Peng He

Department of Chemical and Materials Engineering, University of Cincinnati, Cincinnati, OH 45221, USA

Received: July 21, 2004

Abstract. Nanomaterials such as nanoparticles and nanotubes can be surface functionalized for many novel engineering applications. In bio-probe applications, a functional group can be deposited on magnetic nanoparticles. The deposited thin film can provide appropriate chemical bondings for the attachment of antigen and DNA in instant food test. Nanotubes have been widely used in polymer composites. Due to their high surface energies, nanotubes can severely cluster and in turn degrade the mechanical properties. Coating of a thin polymer film on nanotube surfaces can greatly enhance dispersion and interfacial bonding, resulting in significantly improved strength/nanotubes are desired that can be applied to model systems for both fundamental study and practical applications. In this paper, experimental results on the deposition of polymer films on various nanoparticles and nanotubes are presented. High-resolution transmission electron microscopy (HRTEM), time of flight secondary ion spectroscopy (TOFSIMS), and infrared (FTIR) has been performed to characterize the coated and uncoated nanopaticles and nanotubes. Fundamental deposition mechanisms involving interfaces and related properties are also presented.

1. INTRODUCTION

The development of surface nanostructures will be one of the key engines that drives our technological society in the 21-century. This rapidly growing area focuses on tailoring a nanoparticle surface structure for specific and unique properties. The 'nano-scale' engineering has produced such materials as layered composite semiconductors for high speed electronic devices, blue lasers and diodes and vertical cavity lasers that read and write our CDs, and highly conductive, but low loss thin films for panel displays.

Although, nanoparticles and nanotubes are used in many applications because of their desirable bulk properties [1,2], the surface of the nanotubes is often not ideal for the particular application. The ability to deposit well-controlled coatings on nanotubes would offer a wide range of technological opportunities based on changes to both the physical and chemical properties of the nanotubes. Atomic layer controlled coatings on nanotubes, for example, would allow nanotubes to retain their bulk properties but yield more desirable surface properties. These ultrathin coatings could act to activate, passivate or functionalize the nanotubes to achieve both desirable bulk and surface properties.

In these applications, the nanostructure involves an ultrathin film on the nanoparticle surface that can also be tailored into multilayers by a unique plasma technique. Both the substrate nanoparticle and the ultrathin film serve certain functionalities for specific applications. In panel display, the substrate must be a low-loss nanoparticle for visible light with a highly conductive thin film uniformly deposited in its surface. All these functionalities are required in penal display applications and can be best achieved by the plasma technique. Nanophase polymers typically consist of a hard phase dispersed in a soft phase to achieve specific enhanced properties. Silica, clay or another 'hard' nanoparticle serves as

Corresponding author: Donglu Shi, e-mail: donglu.shi@uc.edu

the hard phase. By manipulation of the physical, chemical and optical properties of the 'hard' phase nanoparticles, tunable materials properties can be achieved. A key aspect of being able to manipulate the properties of the nanoparticles is the surface treatment of the nanoparticles by various processing techniques. This technology produces high-tech properties with the low cost normally associated with plastics.

Another example is the low-temperature consolidation of ceramics at low temperatures via a so-called nanoglue. When an adhesive thin film is coated on the nanopartcle surfaces, these particles can be consolidated at a temperature well below the sintering temperature. However, this method requires the adhesive thin film to be extremely thin and uniform. Therefore the volume percent of the polymer is limited to only a few percent. In this way, the bulk mechanical properties of ceramics can be maintained.

Therefore, tailoring the nanoparticle surface structure becomes of ultra importance in today's nanotechnology. The broad range of these properties due to nano surface structures include electromagnetic conductivities, uniformity, index of refraction, high reflectance, low absorption, stress, and the adhesion of the film structure to the substrate. All these properties are determined by new parameters such as interfaces between the ultrathin film and the nanoparticle, nanoparticle surface morphology, and structures of the film. However, these properties are not well understood as the new nano-surface structures are still being developed. Thus, it is essential to establish a fundamental understanding of the structure-property relationships for the surface-tailored nanoparticles.

In current research of nanomaterials, it has become critical to modify the surfaces of the nanoparticles for both fundamental research and engineering applications [1-8]. Taking different film technologies into consideration, plasma polymerization coating as well as plasma surface treatment of powders is particularly promising because of the following unique features and advantages. (1) The starting feed gases used may not contain the type of functional groups normally associated with conventional polymerization; (2) Such films are often highly coherent and adherent to a variety of substrates, including conventional polymers, glasses and metals; (3) Polymerization may be achieved without the use of solvents; (4) Plasma polymer films can be easily produced with thickness from several nanometers to 1ìm; (5) through careful control of the polymerization parameters, it is possible to tailor the films with specific chemical functionality, thickness, and other chemical and physical properties.

In this paper, we present experimental results on several important areas including coating acrylic acid (AA) for ion exchange, coating of polymer thin films on magnetic nanoparticles for bio probes, and surface modification of carbon nanotubes in polymer composites. HRTEM, TOFSIMS, and FTIR experimental results are also presented on the characterization of coated polymer thin films.

2. EXPERIMENTAL DETAILS

The plasma-coating facility is a homemade system. The schematic diagram of the plasma reactor for thin film deposition of nanoparticles is shown in Fig. 1. It consists mainly of a radio frequency (rf) source, the glass vacuum chamber, and press gauge. The vacuum chamber of plasma reactor has a long Pyrex-glass column about 80 cm in height and 6 cm in internal diameter [9–11]. The powder is vigorously stirred at the bottom of the tube and thus the surface of particles can be continuously renewed and exposed to the plasma for thin film deposition during the plasma polymerization processing. A magnetic bar was used to stir the powders. The gases and monomers were introduced from the gas inlet

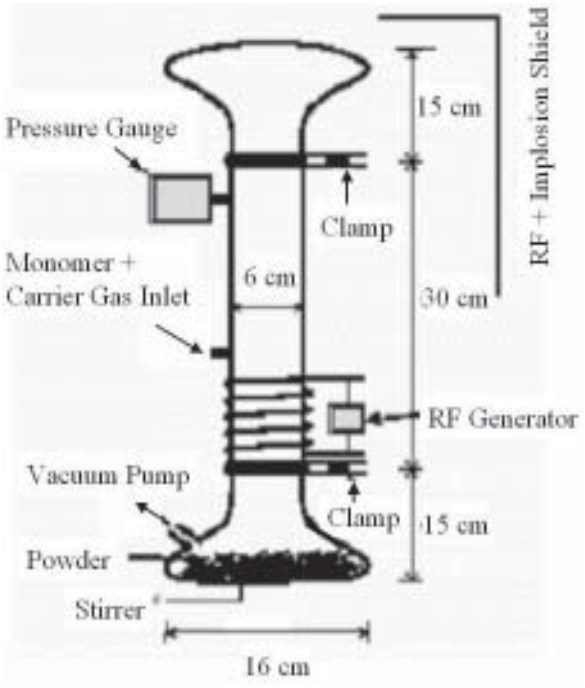

Fig. 1. The plasma reactor for thin film coating of the nano-particles.

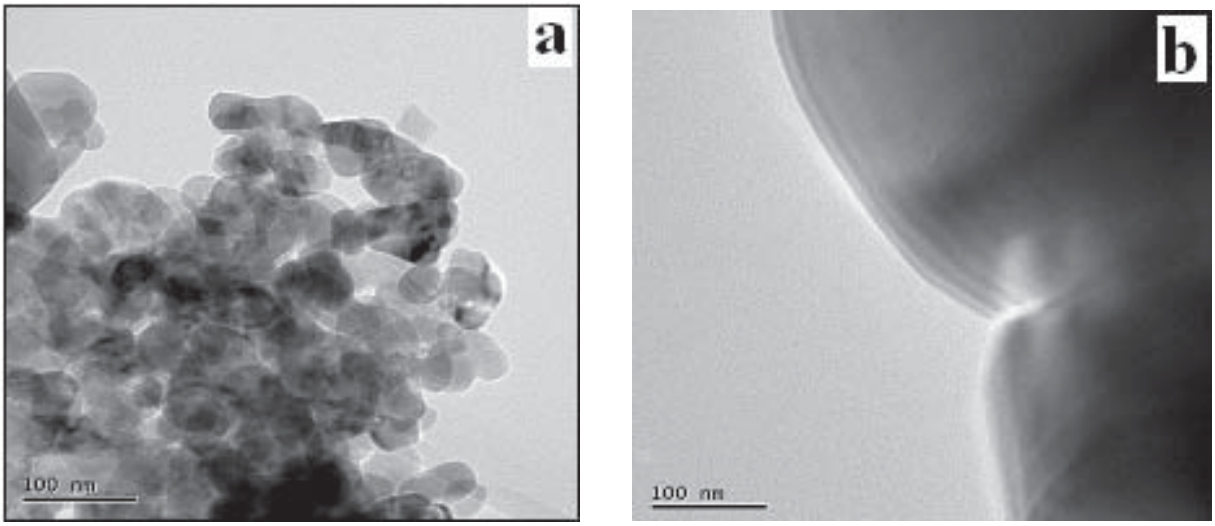

Fig. 2. TEM images of uncoated ZnO at different magnifications.

during the plasma cleaning treatment or plasma polymerization. Before the plasma treatment, the basic pressure was pumped down to less than 50 mtorr and then the carrier gas (such as argon) or monomer vapors were introduced into the reactor chamber. The operating pressure was adjusted by the gas/monomer mass flow rate. During the plasma polymerization processing, the input power was 10-80 W and the system pressure was 300-450 mtorr. The plasma treatment time was 15 to 120 minutes according to the different monomers and the different film thickness desired.

After the plasma treatment, the treated powders were characterized by using Transmission Electron Microscopy (TEM), Secondary Ion Mass Spectrometry (TOFSIMS), and Infrared (FTIR). The high-resolution TEM (HRTEM) experiments were performed on a JEOL JEM 4000EX TEM.

In this research, the substrates used for plasma deposition include ZnO, $NiFe_2O_4$, $YYbErO_2S$, and carbon Nnnotubes. The ZnO nanoparticles are commercial products from the Zinc Corporation of American in Monaca, PA. The $NiFe_2O_4$ nanoparticles are purchased from the Inframat Corporation in Willington, CT. The $YYbErO_2S$ nanoparticles are synthesized by the OraSure Technologies, Inc in Bethlehem, PA. The carbon nanotubes (Pyrograf-III PR-24) are from Applied Science Inc located in Cedarville, Ohio. The monomers, such as pyrrole, acrylic acid, and C_6F_{14}, styrene are provided by Alfa Aesar, A Johnson Matthey Company, Ward Hill, MA.

3. RESULTS AND DISCUSSION

3.1. Coating of acrylic acid films on ZnO nanoparticles

We explored different polymer films such as acrylic acid (AA) on ZnO by the novel plasma treatment [12,13]. Such a coating can be used in ion exchange experiment for removal of metallic ions in water. Fig. 2 shows the TEM images of uncoated ZnO nanoparticles. Several features can be seen from these images. First, as can be seen, the size of these particles has a large distribution ranging from 20 nm and over 100 nm. Second, the surfaces of these particles are rather smooth without any foreign impurities. Third, they are mostly irregularly shaped and not spherical like. Figs. 3a to 3d are the bright field images of the coated ZnO nanoparticles at different magnifications. Figs. 3a and 3b show the low-magnification of a ZnO particle coated with acrylic acid (AA) film. As can be seen, the coating is uniform all the way on the entire surface of the particle. In our TEM observation, we found that, although these particles have different diameters, the film remains the same thickness indicating a uniform distribution of active radicals in the plasma chamber. Figs. 3c and 3d are the images at higher magnifications. The uniformity of the AA thin film can be clearly seen in these photographs. The film thickness is about 5 nm.

Compared to Fig. 2, a bright thin film was evident around the particles. From HRTEM images,

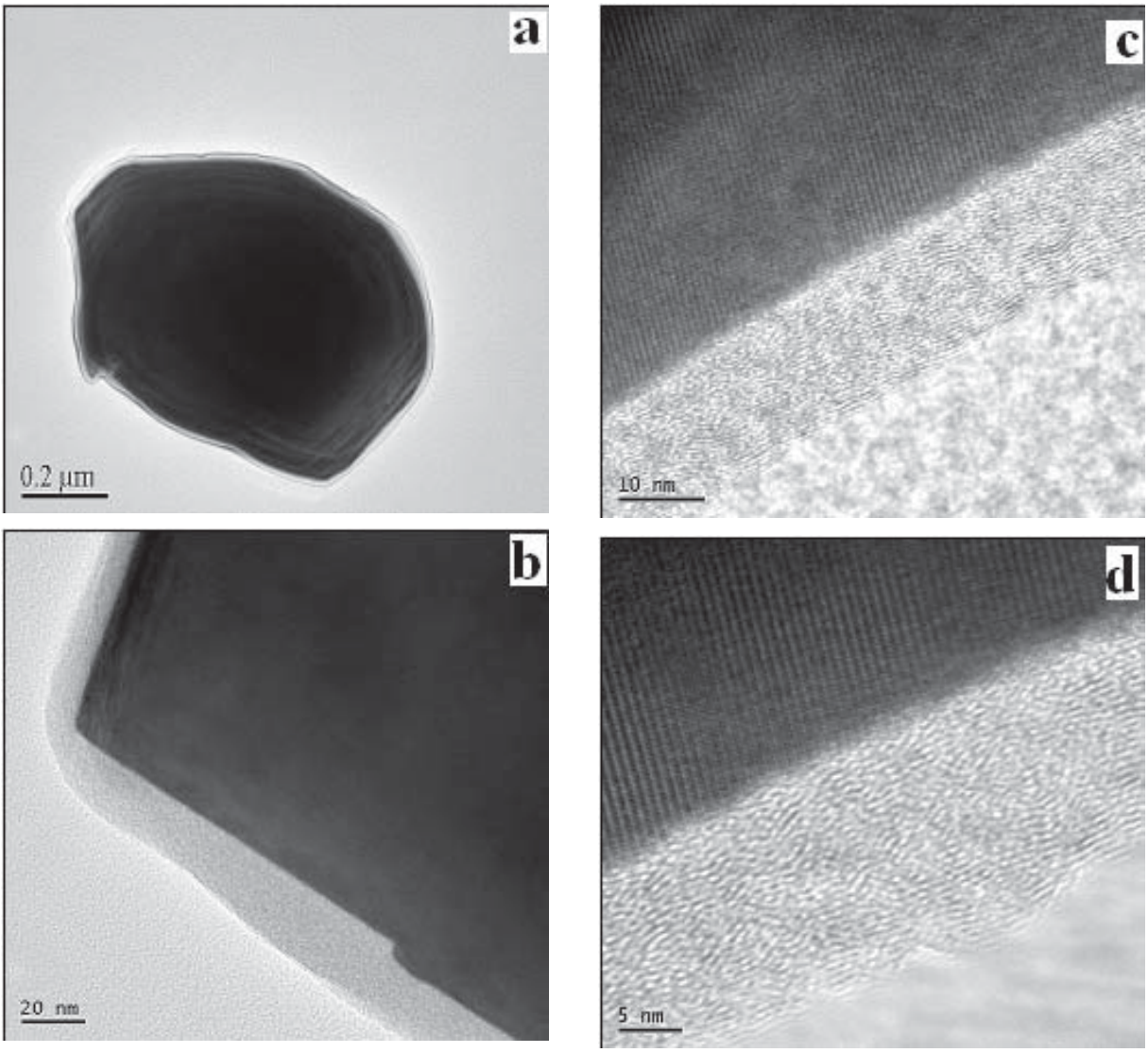

Fig. 3. (a) Bright-field TEM image of the AA-coated ZnO nanoparticles at low magnification. (b) HRTEM image showing the AA-coated ZnO nanoparticle surfaces at higher magnification. (c,d) HRTEM images of AA-coated ZnO showing the amorphous nature of the AA thin film and the crystal lattices of the ZnO structure.

the thin film exhibits an amorphous structure interfacing with the crystalline lattices of ZnO. The coating thickness is approximately 10-20 nm thick over the entire particle surface. Particularly interesting, although the shape of particles is non-spherical, the coating remains the same thickness indicating that the plasma chamber produce a uniform coating on all the particles.

To confirm the TEM observations shown in Figs. 2 and 3, TOFSIMS was carried out to study the surface films of the particles. Figs. 4a and 4b show the positive and negative TOFSIMS spectra of coated ZnO particles. In Fig. 4a one can see that the spectra of the positive ion from the coated ZnO have strong peaks of functional groups such as $C_4H_7^+$, $C_4H_9^+$, $C_6H_{13}O_4$, $C_7H_9COH^+$, and $C_7H_9COOH^+$ indicating a surface coating on the particles consistent with the HRTEM data presented in Fig. 2 and 3. In Fig. 4b, where the spectra of the negative ions are presented, we also see the AA monomer, AA dimer, and AA dimmer + C_2H_4 and AA dimmer + C_3H_6, which are strong indications of these functional groups. These are the typical characteristic cluster patterns of a plasma-polymerized poly(acrylic acid) film.

FTIR was used to study the effect of the plasma power on the molecular structure of the AA films. As can be seen in Fig. 5a, the strong C=O peak near 1700 cm^{-1} indicates the surface coating of the

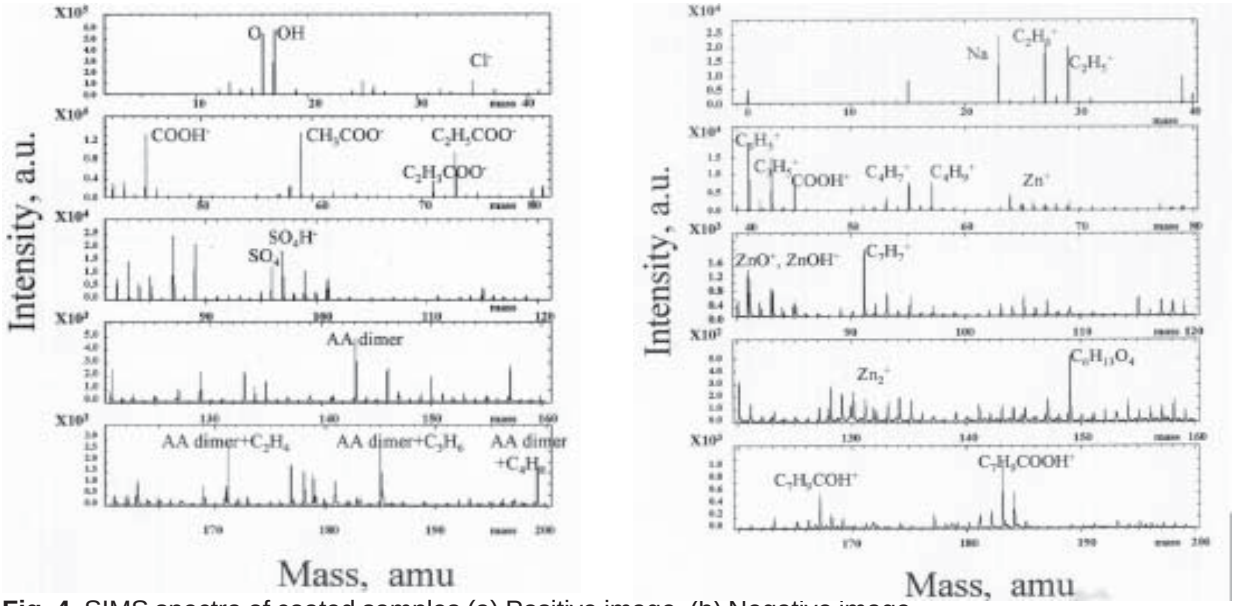

Fig. 4. SIMS spectra of coated samples (a) Positive image, (b) Negative image.

nanoparticles, and it is consistent with the HRTEM data presented in Fig. 3. The peak of C=O intensifies as the plasma power increases up to 80 W, indicating a strong plasma power dependence. The intensity of this peak also indicates an increased amount of C=O function groups that originate from acrylic acid.

In order to investigate the solubility of the plasma film, the coated ZnO powder were immersed into Ni^{+} solution. After 1 h, the sample was removed from the solution, dried, and the FTIR experiment was again performed on the nickel solution treated powder. The results are shown in Figs. 5b, 5c, and 5d. In this figure, we can see that the AA film is

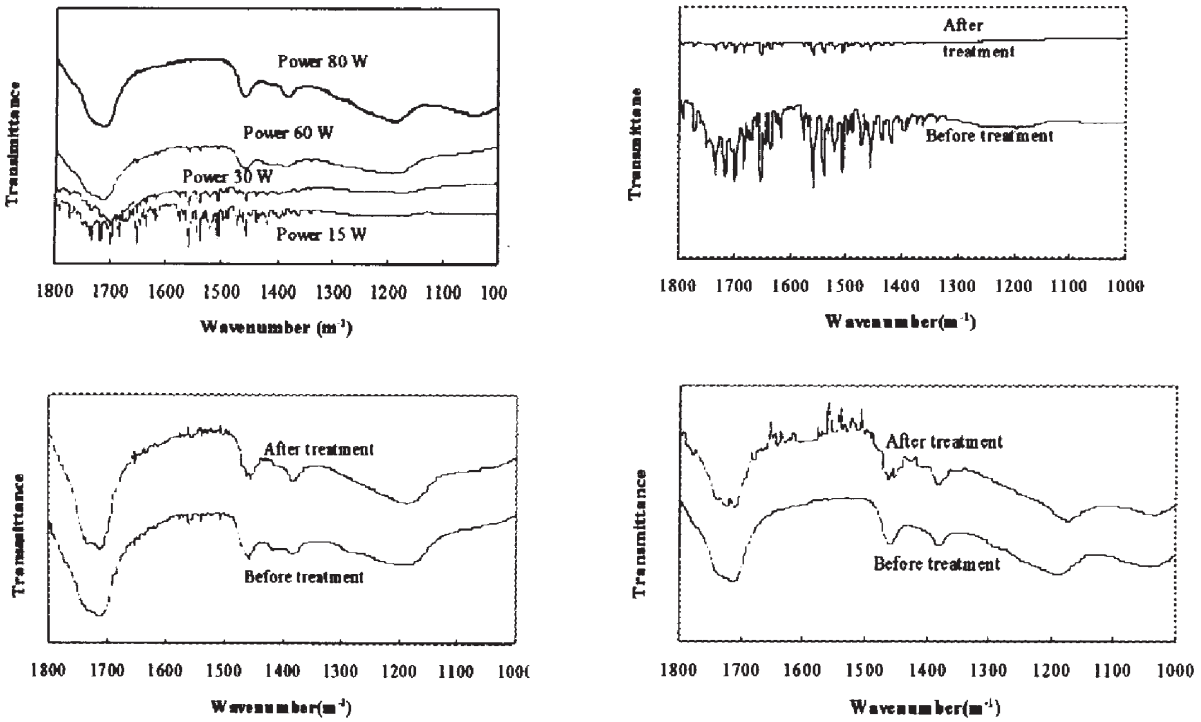

Fig. 5. (a) FTIR spectra of AA-coated ZnO at different plasma powers. The FTIR spectra of Ni solution treated, AA-coated ZnO nanoparticles at plasma power of (b) 15 W, (c) 60 W, and (d) 80 W.

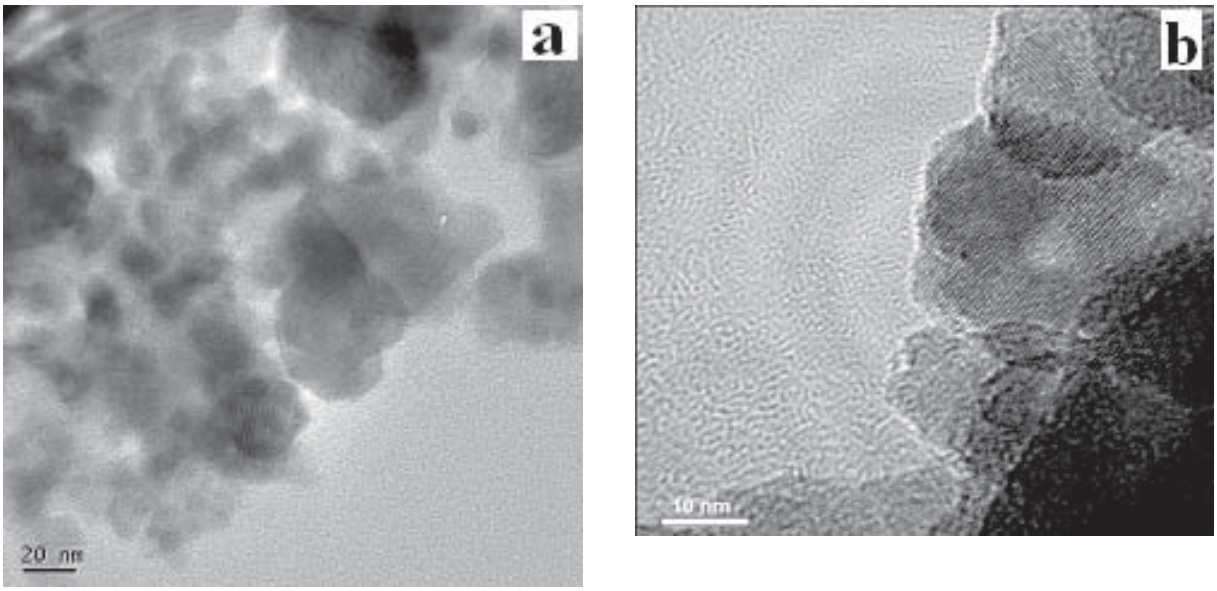

Fig. 6. (a) Bright-field image of the original, uncoated $NiFe_2O_4$ nanoparticles; a particle size distribution ranging from 10–50 nm. (b) HRTEM images of the original $NiFe_2O_4$ nanoparticles showing crystal lattice and the uncoated nature of the nanoparticle surfaces.

entirely soluble 15 W of plasma power. The FTIR spectra clearly show that the film is removed by the nickel solution after immersing for only 1 h. However as the plasma power is increased to 60 W (Fig. 5c) and 80 W (Fig. 5d), the AA film remains after immersion in the nickel solution. This indicates that large cross links exist in the polymer, which prevents the AA film from dissolving in the nickel solution; even that the polymer film has the strong hydrophilic function groups of COOH.

3.2. Plasma coating of magnetic nanoparticles

Fig. 6 shows the HRTEM image of the original, uncoated $NiFe_2O_4$ particles. As can be seen in this figure, the particle size ranges around 10-50 nanometers and they are severely aggregated together. Fig. 6c is the HRTEM image of the original $NiFe_2O_4$ nanoparticles. The lattice image further reveals the crystallographic features of the naked $NiFe_2O_4$ particles.

Fig. 7 shows the HRTEM images of coated $NiFe_2O_4$ nanoparticles. Quite similar to the coating results on ZnO shown in Fig. 2, the deposited thin films are extremely thin (~1 nm) and uniform on the nanoparticles. However, the magnetic particles are severely clustered resulting in certain difficulties in separating them for complete coating. A mechanical stirrer has been designed to mix the nanoparticles within the glass chamber. The study on the dispersion of magnetic particles is under way.

FTIR experiments have been carried out to characterize the coated magnetic nanoparticles. In Fig. 8, the FTIR spectrum exhibits several strong peaks between 1400 cm^{-1} and 1600 cm^{-1}, which are identified as the C-C vibrating absorption of the benzene ring. These peaks are clear indications of the benzene rings in the plasma polymer structure. In the FTIR absorption spectrum, the range from 690 cm^{-1} to 900 cm^{-1} belongs to the benzene C-H out of plane bending.

As can also be seen in Fig. 8, the peaks at 758 cm^{-1} and 700 cm^{-1} are the special absorption for one hydrogen atom on benzene ring substituted by other function groups. The spectrum shown in Fig. 8 is more complicated than the regular FTIR spectra of polystyrene, but the special absorption peaks for styrene is almost same as regular polystyrene. This implies that, in plasma polymerization, the molecular structure is destroyed by ion or electron bombardment, but the deposited film maintains some polystyrene molecular structure for high compatibility with polystyrene matrix.

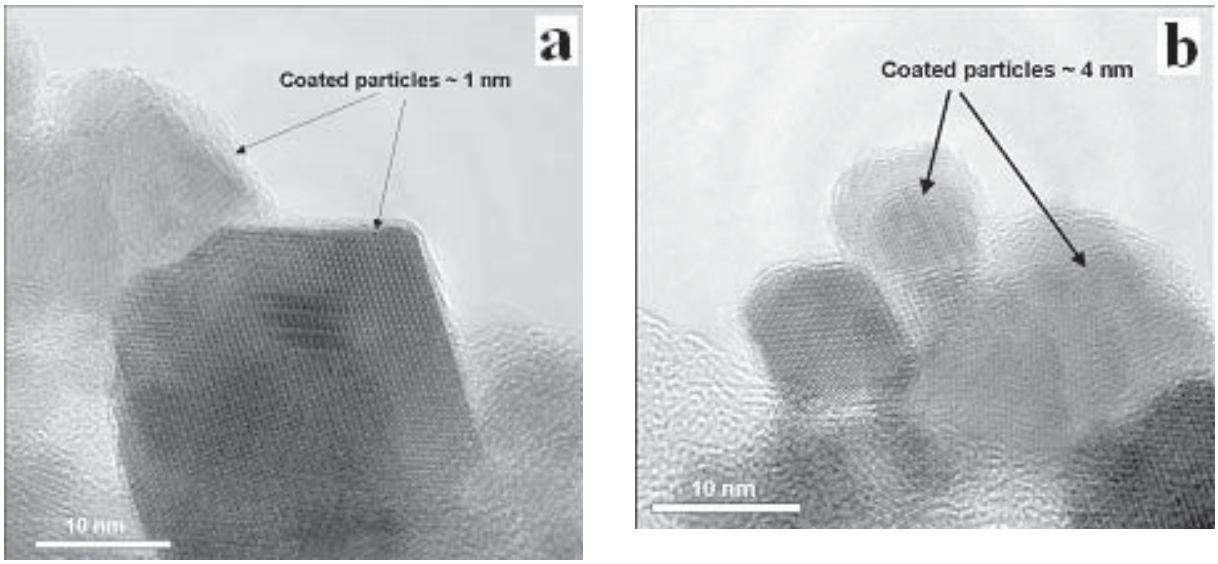

Fig. 7. TEM image of coated $NiFe_2O_4$ at different resolutions.

3.3. Polymer Composites with Coated Carbon Nanotubes

Coating of carbon nanotubes (CNT) by plasma polymerization has also been carried out. The starting CNT powder is comprised of ropes of tubes held together by van der Waals forces. The nanotubes have been coated using polystyrene [14,15]. We used commercial Pyrograf III carbon nanotubes (CNT's) as substrates. The Pyrograf III nanotubes are 70-200 nm in diameter, 50-100 micron long multi-wall carbon nanotubes (Fig. 9). Styrene is used as the monomer for the plasma polymerization. An ultrathin film amorphous layer can be clearly seen covering both the inner and outer surfaces of the

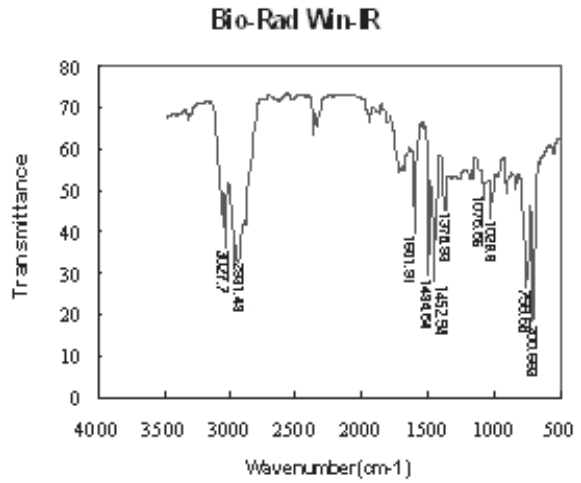

Fig. 8. FTIR spectra of the coating of $NiFe_2O_4$ nanoparticles.

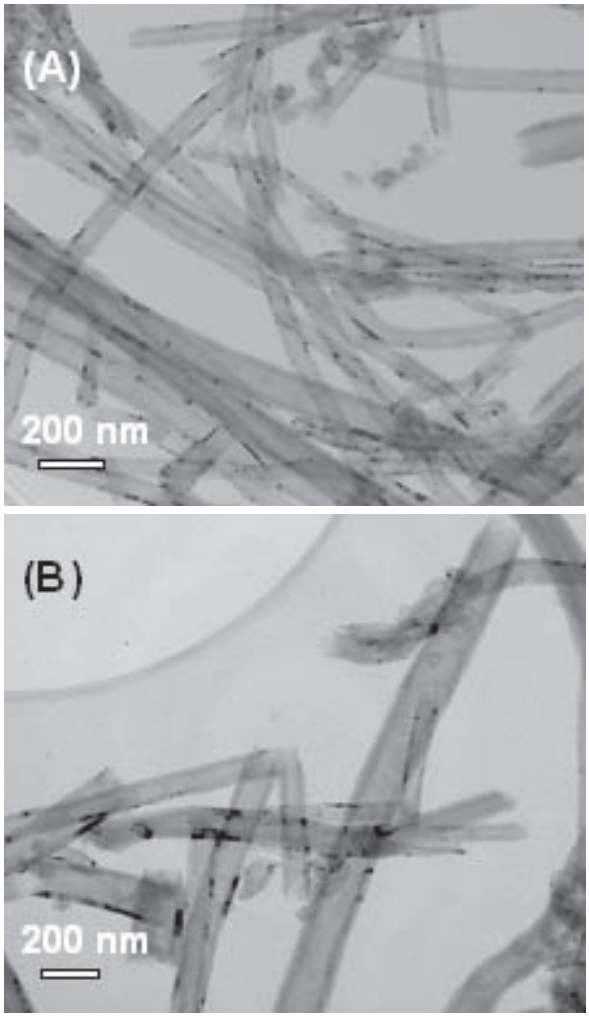

Fig. 9. TEM images of uncoated carbon nanotubes of Pyrograf III PR-24-HT (a); and Pyrograf III PR-24-PS (b).

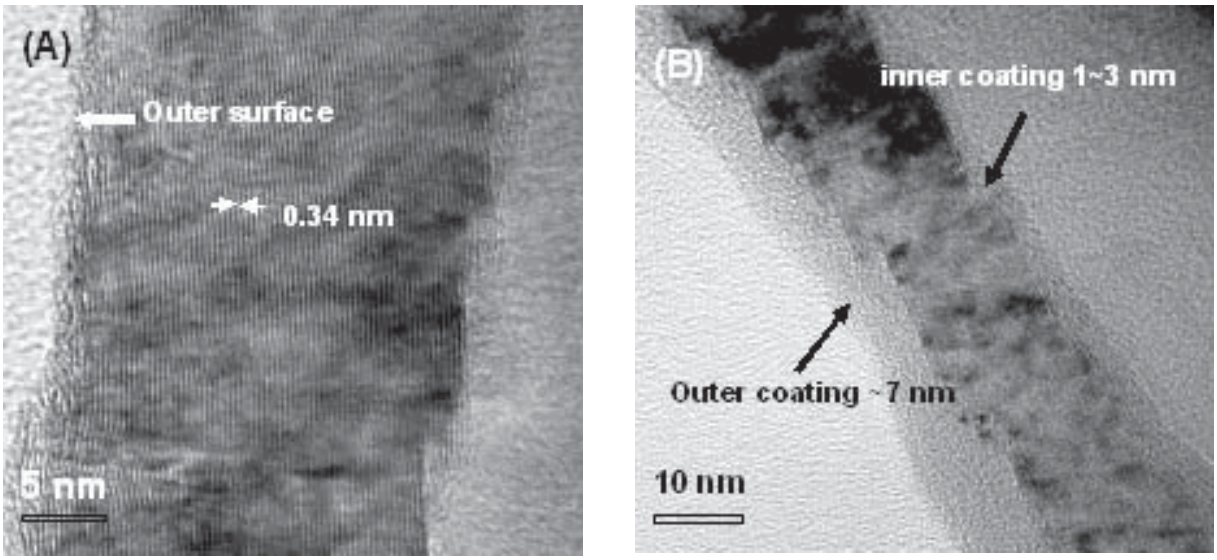

Fig. 10. HRTEM images of Pyrograf III PR-24-PS nanotube: (a) fragments of the wall with inclined planes (002) showing lattice space on the outer and inner surfaces of uncoated Pyrograf III PR-24-PS nanotubes with slight roughness (<1 nm) on the surface; (b) an ultrathin film of pyrrole has been coated on both outer and inner surfaces of Pyrograf III PR-24-PS nanotubes.

nanotubes after plasma treatment (Fig. 10). The thin film is uniform on both surfaces, however, with a larger thickness on the outer wall (10 nm) than on the inner wall (1~3 nm) surface (Fig. 10b). The thickness of ultrathin film is approximately 2~7 nm completely surrounding the nanotube surfaces.

Using these surface modified CNT's, attempt has been made to synthesize polymer composites and study the related mechanical behaviors. Fig. 11a shows the strength as a function of CNT concentration for both coated and uncoated CNT composites. For the uncoated CNT composite, the strength of the composite shows a gradual decrease as the CNT concentration increases while the coated counterpart showed a significant increase in strength. The maximum strength of the coated CNT composite takes place at 3 wt.% and then gradually decreases up to 5 wt.%. The modulus value is shown for both composites in Fig. 11b. A similar trend is seen, which is consistent with the strength values (Fig. 10a). The decrease in properties above 3 wt.% loading may be due to the nanotubes not being initially as well dispersed, and due to later agglomeration of the nanotubes in the matrix. It is anticipated

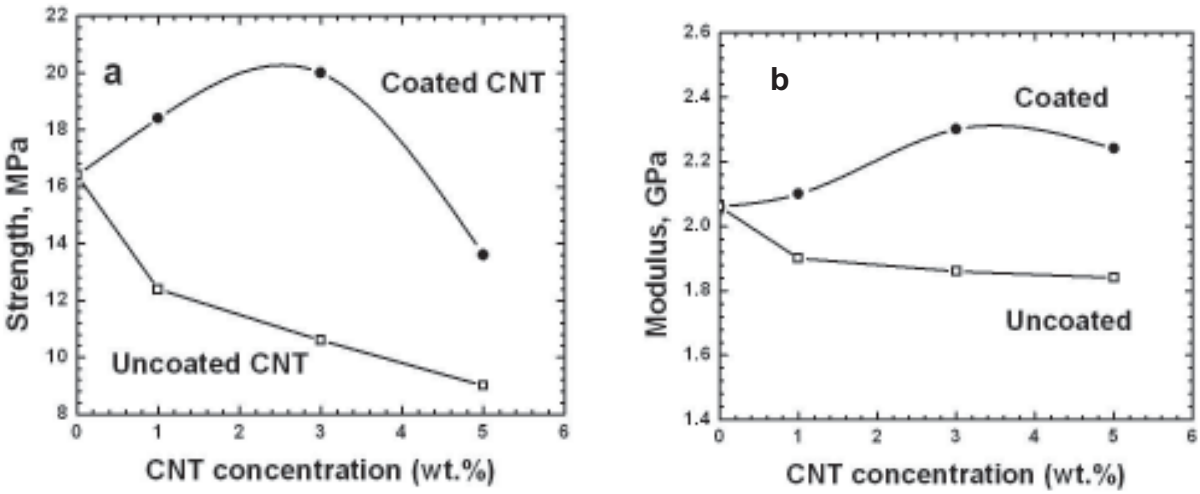

Fig. 11. (a) Strength versus CNT concentration,(b) Modulus versus CNT concentration for both coated and uncoated CNT composites.

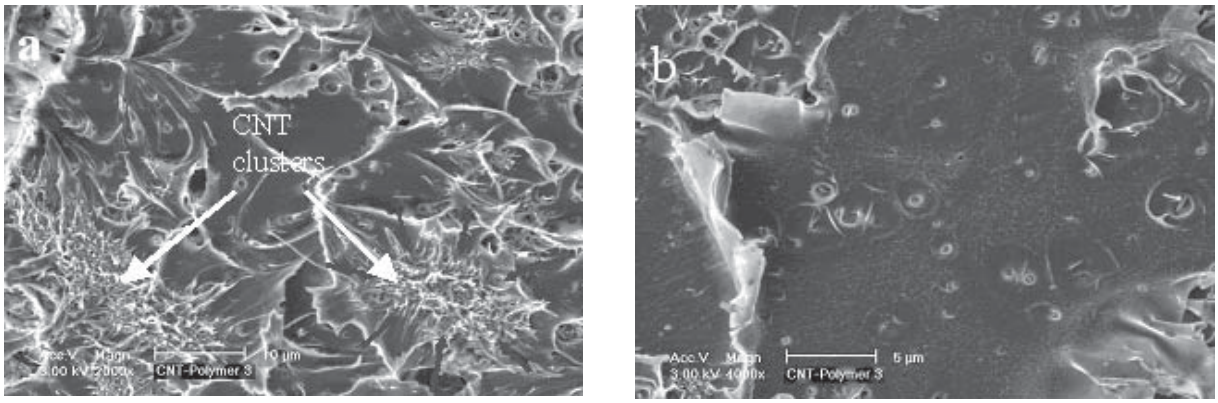

Fig. 12. SEM images showing (a) CNT clusters, and (b) the flat fracture surface of uncoated CNT composite.

that the composite properties will monotonically increase with the wt.% loading of nanotubes if the dispersion can be improved and maintained.

Fig. 12 shows the fracture surfaces of the 3 wt.% uncoated sample. The CNT's are highly clustered in the matrix with approximately a ~10 μm diameter (Fig. 12a), as indicated by the arrows. These clusters appear to be densely distributed with a small spacing of ~25 μm. Another important characteristic of the uncoated CNT composite is the rather flat fracture surface (Fig. 12b) indicating the nature of brittle fracture. At these fracture surfaces severe pullouts of CNTs are also observed. In sharp contrast, the dispersion is greatly improved in the coated CNT composite. Fig. 13 shows the fracture surfaces of the 3 wt.% coated CNT composite. The coated CNT's are well dispersed (Fig. 13a) in the matrix with a wavy type of fracture surface morphology (Fig. 13b). The interface structure between the CNT's and polymer matrix was studied by HRTEM for both coated (Fig. 14a) and uncoated CNT (Fig. 14b) composite samples. The contrast in Fig. 14a clearly shows the coating layer between the carbon nanotube and the matrix, whereas the uncoated carbon nanotube surface is in direct contact with the matrix as shown in Fig. 14b.

The central focus of this part of study is on the enhanced interfacial bonding due to plasma coated thin films on nanotubes. The nature of strengthening in nanotube-reinforced composites is dependent on the stress transfer between the matrix and nanotube. For polymers, tensile loading can produce matrix cracking, nanotube bridging, nanotuber rupture, nanotuber pullout and debonding. In this experiment, pullouts of nanotubes were observed in the uncoated nanotube composite as indicated in Fig. 3d, especially within the cluster regions. As the nanotubes are clustered, the interface area between the matrix and nanotube is greatly reduced leading to significantly lowered strength. Further-

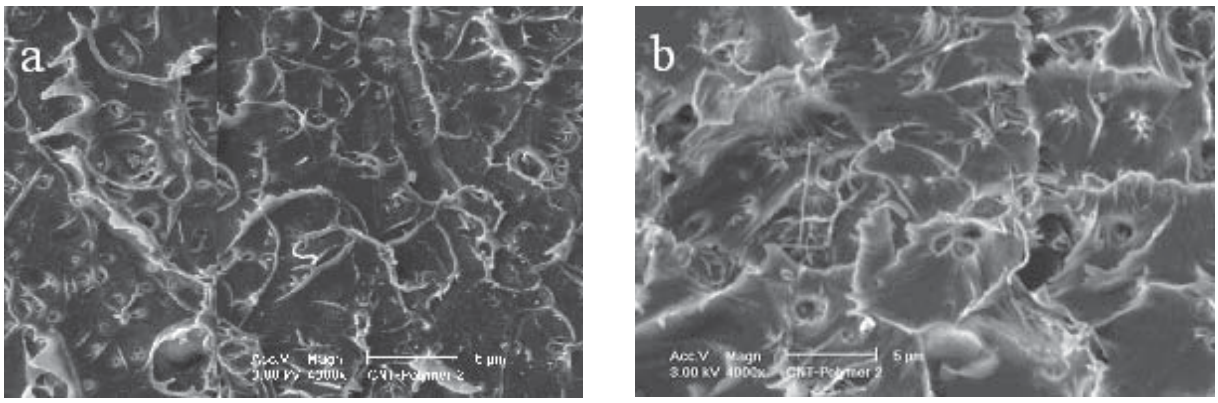

Fig. 13. SEM images showing (a) well dispersed CNT's, and (b) the wavy fracture surface of coated CNT composite.

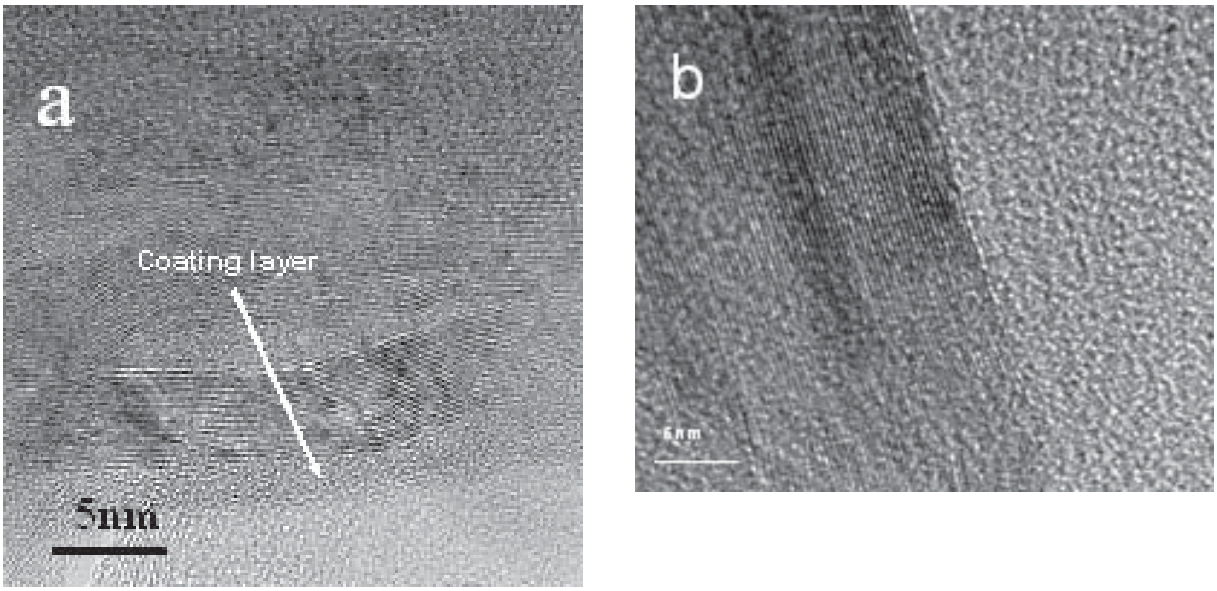

Fig. 14. HRTEM images showing (a) the interface between coated CNT and the matrix, and (b) the uncoated CNT and the matrix.

more, these clusters act as large voids that are responsible for decreasing the strength of the composite as the nanotube concentration increases.

As the nanotube surfaces are modified by plasma coating, the surface energy can be significantly lowered, which can enhance dispersion in the polymer matrix. The well-dispersed nanotubes in the matrix appear to have few clusters and pullouts. In addition, the adhesive film on the nanotube surface, as shown in Fig. 14a, can provide enhanced bonding; and therefore contribute to a considerably increased strength in the coated-nanotube composite. The efficiency of stress transfer is strongly dependent on the maximum value of the shear stress acting at the interface. This stress is also characterized as the interfacial shear strength that depends on the nature of bonding at the interface. As indicated by the interface HRTEM, there is clearly an interfacial adhesion layer due to the coated polymer film on the nanotube surface. Although a quantitative measure of the interfacial shear strength has not been conducted, the effect of enhanced bonding is evident from the increased composite strength and fracture surface morphology.

Although polystyrene is brittle, ite can be macroscopically toughened and manipulated to deform via shear yielding by controlling the microstructure. The improvement of toughness of heterogeneous polystyrene systems is mainly contributed by enhancing the strength of craze and thus the craze resistance; or decreasing the concentrated stress. In the coated nanotube composite, the improved interfacial bond strength between the nanotube and matrix due to an adhesive thin film on nanotube surfaces could increase the strength of the craze. Furthermore, the increase of the interfacial adhesion may suppress the production of voids or flaws in the polymer matrix, which might grow into cracks. Thus, the fracture surface of the coated nanotube composite exhibits typical shear yielding behavior. In contrast, in the uncoated nanotube-polymer composite, a rather flat brittle type of fracture surface occurs (Fig. 12b), similar to the fracture surface of pure polystyrene. This behavior suggests that the highly clustered nanotubes in the matrix do not contribute to shear yielding, and the uncoated nanotube-composite shows a brittle fracture feature. Additionally, the uncoated nanotubes may cause the formation of voids (due to nanotube pullouts) and defects. This could lower the stress required for craze initiation and thus decrease the craze resistance, consistent with the observation that the strength of the uncoated nanofiber-composite decreases with the increasing percentage of nanotubes (Fig. 2).

4. SUMMARY

In summary, a novel approach has been developed to modify the surfaces of the nanoparticles and nanotubes by plasma polymerization. For nanoparticles, an extremely thin polymer film has been deposited on nanoparticles with a high degree of uniformity regardless of the particle sizes. Both TOFSIMS and FTIR have been used to characterize the deposited thin films. Based on the results of TOFSIMS and FTIR, the chemical species with in the polymer structures have been identified. For carbon nanotubes, the plasma deposition of thin films has resulted in great enhancement of dispersion and interfacial bonding of CNT's in polymer composites. As a result of plasma coating, carbon nanotubes can be well dispersed in a polymer matrix. Both the fracture behavior and tensile strength data indicate that the well-dispersed CNT's have contributed to enhanced interfacial shear strength, and therefore have increased the overall strength of the material. It is believed that the strength of the CNT composite will be further enhanced based on the identification of the bonding mechanisms and alignment of CNT's in the polymer matrix. Preliminary results on the magnetic alignment of CNTs in the polymer matrix have already been obtained.

ACKNOWLEDGEMENT

The TEM and SEM analyses were conducted at the Electron Microbeam Analysis Laboratory at the University of Michigan. This research was supported in part by Air Force Contract F33615-01-D-5802.

REFERENCES

[1] R.W. Siegel // *Nanostruct. Mater.* **3** (1993)1.
[2] G.C. Hadjipanayis and R.W. Siegel, *Nanophase Materials, Synthesis-Properties Applications* (Kluwer Press, Dordrecht, The Netherlands, 1994).
[3] G.M. Whitesides, J.P. Mathias and C.T. Seto // *Science* **254** (1991) 1312.
[4] C.D. Stucky and J.E. MacDougall // *Science* **247** (1990) 669.
[5] H. Gleiter // *Nanostruct. Mater.* **6** (1995) 3.
[6] *Nanotechnology,* ed. by A.T. Wolde (STT Netherlands Study Center for Technology Trends, The Hague, The Netherlands, 1998).
[7] N. Inagaki, S. Tasaka and K. Ishii // *J. Appl. Polym. Sci.* **48** (1993) 1433.
[8] C. Bayer, M. Karches, A. Mattews and P.R. Von Rohr // *Chem. Eng. Technol.* **21** (1998) 427.
[9] W.J. van Ooij, S. Luo, N. Zhang and A. Chityala, In: *Proceedings International Conference on Advanced Mfg. Technology* (Science Press, New York, 1999), p. 1572.
[10] W.J. van Ooij and A. Chityala, In: *Surface Modification of Powders by Plasma Polymerization,* ed. by K.L. Mittal (VSP, Utrecht, 2000), p. 243.
[11] W.J. van Ooij, N. Zhang and S. Guo, In: *Fundamental and Applied Aspects of Chemically Modified Surfaces,* ed. by J.P. Blitz and C.B. Little (Royal Society of Chemistry, Cambridge, U.K., 1999), p. 191.
[12] D.Shi, P. He, J. Lian, L. M. Wang and W. J. van Ooij // *J. Mater. Res.* **17** (2002) 2555.
[13] D. Shi, J. Lian, P. He, L. M. Wang, W. J. van Ooij, M. Schulz, Y. J. Liu and D. B. Mast // *Appl Phys Lett*, **81** (2002) 5216.
[14] Donglu Shi and W. J. van Ooij // *Appl. Phys. Lett.* **78** (2001) 1234.
[15] Donglu Shi and W. J. van Ooij // *Appl. Phys. Lett.* **81** (2002) 5216.